View metadata, citation and similar papers at core.ac.uk
brought to you by CORE
provided by Elsevier - Publisher Connector

Self-Reproduction of Fatty Acid Vesicles: A Combined Experimental and Simulation Study

Albert J. Markvoort,[†‡△*] Nicole Pfleger,[†¶△] Rutger Staffhorst,[¶] Peter A. J. Hilbers,[†‡] Rutger A. van Santen,[†§] J. Antoinette Killian,[¶] and Ben de Kruijff[¶]

[†]Institute for Complex Molecular Systems, [‡]Biomedical Engineering Department, and [§]Department of Chemical Engineering and Chemistry, Eindhoven University of Technology, Eindhoven, The Netherlands; and [¶]Research Group Biochemistry of Membranes, Bijvoet Institute, and Institute of Biomembranes, Utrecht University, Utrecht, The Netherlands

ABSTRACT Dilution of a fatty acid micellar solution at basic pH toward neutrality results in spontaneous formation of vesicles with a broad size distribution. However, when vesicles of a defined size are present before dilution, the size distribution of the newly formed vesicles is strongly biased toward that of the seed vesicles. This so-called matrix effect is believed to be a key feature of early life. Here we reproduced this effect for oleate micelles and seed vesicles of either oleate or dioleoylphosphatidylcholine. Fluorescence measurements showed that the vesicle contents do not leak out during the replication process. We hypothesized that the matrix effect results from vesicle fission induced by an imbalance of material across both leaflets of the vesicle upon initial insertion of fatty acids into the outer leaflet of the seed vesicle. This was supported by experiments that showed a significant increase in vesicle size when the equilibration of oleate over both leaflets was enhanced by either slowing down the rate of fatty acid addition or increasing the rate of fatty acid transbilayer movement. Coarse-grained molecular-dynamics simulations showed excellent agreement with the experimental results and provided further mechanistic details of the replication process.

INTRODUCTION

One of the central dogmas in the life sciences is that new membranes grow out of existing ones by the coordinated biosynthesis and integration of new membrane components leading to membrane expansion. Subsequent fission and fusion processes allow membranes to be redistributed within a cell. De novo membrane formation is highly unlikely because of the strong tendency of membrane lipids to self-assemble in water, which will prevent the formation of new membranes in the presence of existing ones.

It is a common hypothesis that the first membrane systems in early life were chemically much more primitive than the current complex membrane lipids, and that the bilayers surrounding the ancestor cells were much less stable and more permeable (1–5). It is also assumed that early membranes could form spontaneously from amphipathic molecules. Most of the support for this hypothesis comes from studies on the bilayer-forming properties of free fatty acids. Several fatty acids (e.g., oleic acid) spontaneously assemble into bilayers when dispersed in water near neutral pH. These bilayers are more dynamic and more permeable than the bilayers formed by the now-common membrane glycerolipids in which two fatty acids are attached to the glycerol moiety of a more complex molecule. The bilayer-forming properties of fatty acids make these molecules the simplest mimics of membrane lipids with interesting technological properties for various applications, such as drug delivery.

The molecular basis for bilayer formation of fatty acids is well understood (6–9). At acidic pH all carboxylate groups are protonated and the fatty acids precipitate, whereas at basic pH the carboxylate is fully charged, causing electrostatic repulsion and thereby favoring the well-known micellar organization of these molecules. Around neutral pH (i.e., close to the pK_a of the carboxyl group) this repulsion is decreased and simultaneously intercarboxylate interactions are increased due to hydrogen bonding, causing an apparent decrease in headgroup size. In the framework of the shape-structure concept of lipid polymorphism, the effective overall shape of the molecule becomes more cylindrical, thereby favoring assembly into bilayers.

A few years ago, a remarkable experiment was conducted that further heightened interest in fatty acids as models for membrane biogenesis studies. When a basic concentrated solution of oleate was diluted toward neutrality, bilayers in the form of vesicles of heterogeneous size were formed, as expected (8,10). However, when the experiment was repeated in the presence of preexisting lipid vesicles (oleate or phosphatidylcholine), the rate of formation of new vesicles was greatly increased and the newly formed vesicles had a much more homogeneous size distribution that was closely related to the size of the original seed vesicles (11,12). This so-called matrix effect demonstrated that existing bilayers play a role in the de novo formation of new vesicles, and provided an interesting model system for membrane and vesicle formation and growth.

Submitted May 18, 2010, and accepted for publication June 17, 2010.

△Albert J. Markvoort and Nicole Pfleger contributed equally to this work.

*Correspondence: a.j.markvoort@tue.nl

Editor: Hagan Bayley.

© 2010 by the Biophysical Society

0006-3495/10/09/1520/9 $2.00

doi: 10.1016/j.bpj.2010.06.057

Several studies (13–27) addressed the mechanism underlying the matrix effect and demonstrated that the fatty acids that originate from the initial micellar solution must first interact with the existing vesicles. However, the precise mechanism remained obscure and various pathways have been proposed. These pathways can be divided into two groups. In the first group, the seed vesicles catalyze the formation of new membranes, presumably by surface-directed assembly of micelles into new membrane sheets that then grow and close up into new vesicles. In the second group, which includes growth and fission models, the membrane of the seed vesicles is proposed to grow by the uptake of the fatty acid micelles, followed by some sort of vesicle division.

Support for the fission mechanism was obtained by cryotransmission electron microscopy experiments with ferritin-entrapped seed vesicles in which the final suspension contained a large amount of ferritin-containing vesicles that were somewhat smaller than the preformed ones (14). On the other hand, evidence for the formation of new vesicles was provided by Chen and Szostak (15), who showed, using kinetic experiments and fluorescently labeled fatty acids, that part of the added fatty acids do form new membranes as the dye molecules in the membranes of the seed vesicles are only partially diluted.

In this study we combined experimental approaches with coarse-grained (CG) molecular-dynamics (MD) simulations to derive, in molecular detail, a pathway for the vesicle replication process. In particular, we show that the membranes of the seed vesicles grow upon addition of fatty acids, demonstrating their uptake in the membrane. In addition, we show that new vesicles also are formed when fatty acids are added below the critical micelle concentration (cmc), i.e., as monomers, demonstrating that not only micelles give rise to the matrix effect. Experiments in which the rate of addition of fatty acids was varied suggest a mechanism in which the initial imbalance of newly inserted material across the outer and inner leaflets of the seed vesicles is the driving force for fission. The proposed pathway provides a plausible explanation for the matrix effect, with fatty acid transbilayer movement playing a key role in determining the final size of the vesicles.

MATERIALS AND METHODS

Materials

1,2-Dioleoyl-*sn*-glycero-3-phosphocholine (DOPC) was purchased from Avanti Polar Lipids (Alabaster, AL). Potassium oleate was purchased from Sigma Aldrich (Steinheim, Germany). 5(6)-Carboxyfluorescein (CF) was obtained from Molecular Probes (Leiden, The Netherlands). Other chemicals were of the highest quality available.

Preparation of model systems

A thin film of DOPC vacuum-dried from a chloroform solution was hydrated in 0.2 M bicine/NaOH buffer, pH 8.5, to a final phospholipid concentration of 11 mM. Subsequently, the lipid suspension was freeze-thawed 10 times using a water bath at 60°C and an ethanol/dry ice bath. Large unilamellar vesicles (LUVs) were prepared by repeated extrusion of this suspension using Whatman (Maidstone, England) filters with different pore sizes.

In the case of CF-leakage experiments, the DOPC film was hydrated in a solution of 0.2 M bicine/NaOH, 50 mM CF, pH 8.5. After extrusion, the CF-containing vesicles were centrifuged for 1 min at 1620 × *g* through a Sephadex G25 spin column equilibrated with 0.2 M bicine/NaOH, 100 mM NaCl, pH 8.5, to remove the nonenclosed CF.

Fatty acid seed vesicles were prepared by adding 0.3 mL of a 22 mM micellar oleate stock to 1.9 mL bicine buffer, pH 8.5. The vesicles formed by dilution to the buffer at pH 8.5 were then extruded 10 times through a 200 nm Whatman filter.

Oleate micelles were formed by dissolving the fatty acid in deionized water to a final concentration of 22 mM, resulting in a pH of 10.5. Unless indicated otherwise, all procedures and experiments were carried out at room temperature.

For the formation of fatty acid vesicles without the presence of seed vesicles, 0.6 mL of a 22 mM micellar oleate solution at pH 10.5 was added to 2.2 mL 0.2 M bicine buffer, pH 8.5. In the case of DOPC seed vesicles, 0.3 mL DOPC LUV 200 nm (11 mM) were diluted with 1.9 mL of bicine buffer and then mixed with 0.9 mL of a 22 mM micellar oleate solution at pH 10.5. Experiments in the presence of oleate seed vesicles were performed by mixing 2.2 mL of those seed oleate vesicles with 0.9 mL of the 22 mM micellar oleate solution.

For the experiments of oleate addition below the cmc, oleate (22 mM) was diluted with water_NaOH (pH 10) to 0.2 mM. Then 1 mL DOPC LUV 150 nm (0.1 mM) was added to 1 mL of this 0.2 mM oleate solution.

Turbidity measurements

The optical density was recorded online at a wavelength of 400 nm in a Perkin Elmer UV/Vis Lambda 18 spectrometer, using a quartz cell with a path length of 1.0 cm and an integrated stirring device.

Measurement of size distribution

The size of the vesicles was measured with the use of a Malvern 3000 Zeta sizer. The scattering was measured at an angle of 90° at 25°C. The viscosity and diffraction indexes were set to water (0.83 and 1.33). For size analysis, the monomodal algorithm was applied.

Variation of the rate of addition of oleate micelles

In the case of slow addition, a 22 mM micellar oleate solution at pH 10.5 was added to 0.2 mL DOPC LUV 200 nm (11 mM) at a rate of 0.06 mL/h for 10 h. The addition rate was carefully controlled by means of a pump.

Leakage experiments

CF leakage from the vesicles was measured by fluorescence spectroscopy using an Aminco SPF-500 C spectrofluorometer at an emission and excitation wavelength of 515 and 492 nm, respectively. At time point 1, 0.2 mL DOPC LUV 200 (11 mM PC) loaded with 50 mM CF was added to 0.9 mL 0.2 M bicine buffer, 100 mM NaCl, pH 8.5. At time point 2, 0.3 mL 22 mM oleate, pH 10.5, was added. At time point 3, the vesicles were lysed by addition of 10% TX-100.

MD simulations

All calculations were performed on a Rocks Cluster located at the Eindhoven University of Technology. This cluster comprises 32 nodes, each containing

two Dual Core AMD Opteron(tm) processors and 4GByte of memory. The PumMa program was used to run CG MD simulations on 24 cores in parallel. In the CG model used (which is based on the CG lipid model we used previously to study spontaneous formation (28), fusion (29), deformations (30,31), and fission (32) of phospholipid vesicles), three types of particles are present: T particles that represent the apolar tails, H particles that represent the polar headgroups, and W particles that describe the solvent (water). One fatty acid is described by a linear chain of two H particles and four T particles (see Fig. 5 *A*). One W particle represents four water molecules.

Three potentials (bonded, nonbonded, and bending) are defined in the force field. The bonded one is used for particles that share a bond, whereas the nonbonded one is used for interactions between all other pairs of particles. The bending potential is used to add rigidity to the molecules. All parameters used in the CG model are expressed in reduced units (28). Bonded interactions are described by a harmonic potential with force constant of 325.0 and an equilibrium bond length of 1.051. Hydrocarbon chains are rather flexible; however, the anticonformation is energetically favorable. To mimic this behavior, some rigidity is incorporated by means of a cosine harmonic bending potential between T particles with a force constant of 16.0 and an equilibrium angle of 180°. The nonbonded interactions are governed by so-called truncated shifted Lennard-Jones potentials. These nonbonded interactions can be divided into two categories: hydrophilic-hydrophilic and hydrophobic-hydrophobic interactions on the one hand, and hydrophilic-hydrophobic interactions on the other hand. For the first category a cutoff radius of 2.5 times the collision diameter is used, whereas for the second category the potential is cut off at the minimum, such that only the repulsive part remains. For these repulsive potentials (T-W and T-H), as well as for the T-T interaction, the characteristic energy (ε) in the Lennard-Jones potential is set to 1.0. For the W-W interaction this value is 1.88. In contrast to the original model, where all hydrophilic-hydrophilic interaction had the same strength, here the G-G and the G-W interactions have a 5% lower and 5% higher strength, respectively (i.e., $\varepsilon_{G\text{-}G} = 1.768$ and $\varepsilon_{G\text{-}W} = 1.974$). This choice for the interactions slightly increases the hydration of the headgroups, mimicking the expected behavior because the headgroups of the fatty acids are partly charged, in contrast to those of neutral phospholipids, and will thus repel each other to some extent.

RESULTS

Matrix effect

The essence of the original matrix effect (11,12) is illustrated by the results in Fig. 1 and Table 1. Fig. 1 shows turbidity measurements upon dilution of oleate micelles at high pH toward neutrality. In the absence of seed vesicles, this leads to a slow increase in turbidity (trace *A*), as observed previously (23). However, in the presence of 200 nm seed vesicles of either DOPC (trace *B*) or oleate (trace *C*), the turbidity increase is very fast and reaches steady-state levels within minutes upon addition of an excess of oleate.

The final vesicle size was related to the size of the seed vesicles as determined by dynamic light scattering (DLS) (Table 1). In the absence of seed vesicles, the newly formed oleate vesicles have an average diameter of 430 nm with a high polydispersity index, indicating a highly heterogeneous vesicle size. Upon addition of excess oleate to either 100 or 200 nm DOPC vesicles or to 200 nm oleate seed vesicles, the size distribution becomes less homogeneous but the average size of the vesicles remains almost conserved. This

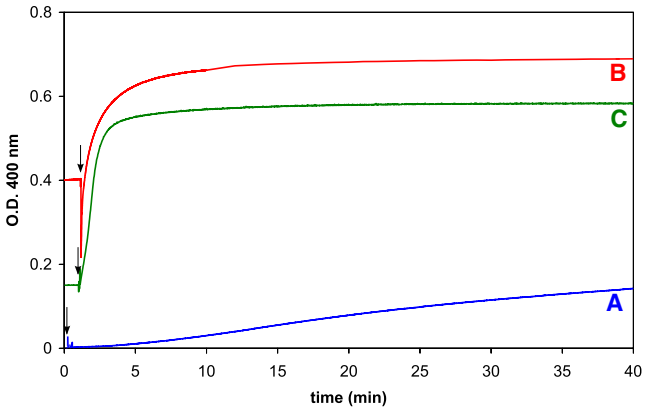

FIGURE 1 Effect of the presence of seed vesicles on the turbidity increase caused by dilution of oleate micelles toward neutrality. A micellar oleate solution of pH 10.5 was added at the time point indicated by the arrow to a bicine buffer at pH 8.5 in the absence (*A*) or presence of 200 nm DOPC vesicles (*B*) or 200 nm oleate vesicles (*C*). The amount of oleate added resulted in an overall fourfold increase in the number of chains already present in *B* and *C*.

conservation of the size occurs in spite of the considerable membrane expansion caused by the addition of an excess of oleate to obtain an overall fourfold increase of the amount of fatty acid chains. Hence the results demonstrate that oleate causes the formation of more vesicles with on average a similar size as the seed vesicles. Thus, in these experiments we were able to reproduce the original matrix effect (11,12) using very simple and homogeneous fatty acid/lipid systems in which no acyl chains other than oleate were present.

The permeability barrier of the seed vesicles remains intact during the formation of new vesicles

To gain further insight into the molecular nature of the process responsible for the matrix effect, we analyzed the barrier properties of the vesicles upon oleate addition by enclosing the fluorescent dye CF at self-quenching concentrations in the seed vesicles.

Fig. 2 shows a typical online fluorescence recording of CF loaded 200 nm DOPC vesicles. Upon addition of the

TABLE 1 Vesicle size analysis by DLS of samples 30 min after oleate micelles were diluted toward neutrality in the absence or presence of seed LUVs extruded through filters with pore sizes of 200 nm or 100 nm

Seed vesicles	Before oleate addition		After oleate addition	
	ø (nm)	PI	ø (nm)	PI
—	—	—	430	1
DOPC	203	0.09	186	0.20
DOPC	97	0.09	72	0.20
Oleate	204	0.10	215	0.21

Diameter of the vesicles is presented together with the polydispersity index (PI). Experimental conditions were identical to those in Fig. 1.

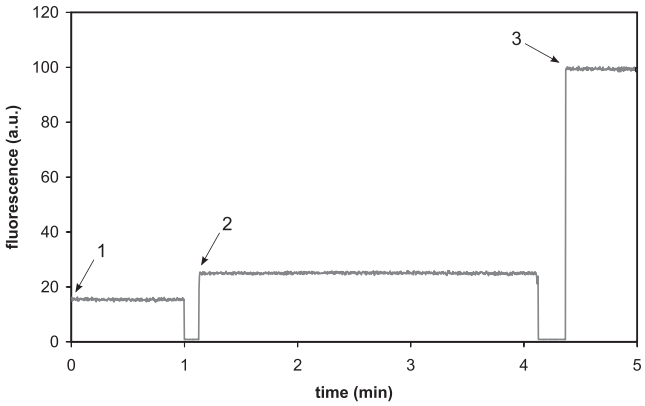

FIGURE 2 Effect of dilution of oleate micelles toward neutrality on CF leakage of 200 nm DOPC seed vesicles. Time point 1 shows the relative fluorescence intensity of a dispersion of DOPC vesicles loaded with CF at a self-quenching concentration. At time point 2, an excess of oleate pH 10.5 was added, such that the final number of chains was 2.5 times greater than the number before oleate addition. At time point 3 the vesicles were lysed by 10% TX-100. The signal drop to zero occurred when the cuvette was removed from the spectrofluorometer for the addition of oleate or TX-100.

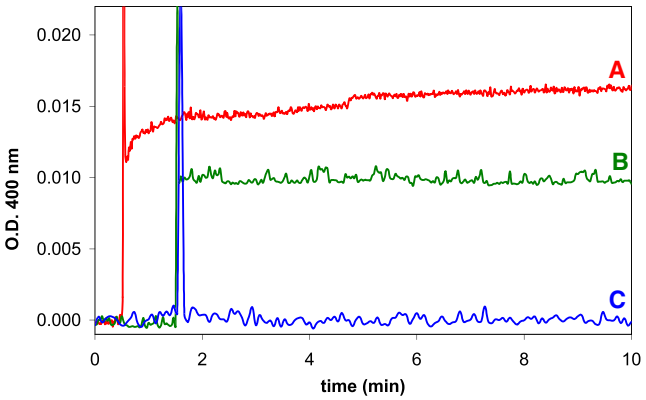

FIGURE 3 Turbidity measurement of fatty acid addition below the cmc: (*A*) Addition of 1 mL of 150 nm DOPC (0.1 mM) vesicles (pH 8.5, bicine buffer) to 1 mL of a 0.2 mM oleate solution of oleate monomers. (*B*) Control measurement of addition of 1 mL of 150 nm DOPC (0.1 mM) vesicles (in bicine buffer, pH 8.5) to 1 mL water. (*C*) Control measurement of dilution of 1 mL of a solution of oleate monomers with 1 mL of bicine buffer, pH 8.5. The final pH is 8.5 due to the buffer.

vesicles to the buffer (time point 1), very little fluorescence is observed, probably due to the binding of some residual CF to the outside of the vesicles. The signal is stable in time, indicating that the vesicles are not leaky. The addition of an excess of oleate at pH 10 (time point 2) leads to a small increase of fluorescence. Control experiments in which an equivalent amount of water adjusted to the same high pH was added instead of the oleate micelle solution suggested that this increase is caused by a pH change and not by leakage of the dye to the exterior. Only when the vesicles were disrupted by addition of Triton X-100 (time point 3) was a rapid efflux of CF observed. Similar results were obtained when oleate vesicles were used as seed vesicles, although in these vesicles less of the CF could be enclosed because by themselves such vesicles are more permeable (4,5). Thus, we conclude that the formation of new vesicles upon addition of oleate to seed vesicles is a nonleaky process. This is consistent with previous findings from studies using different vesicle systems and less quantitative electron microscopy techniques (14). As a final control, light scattering and DLS confirmed that CF enclosure did not affect the process of formation of new vesicles after oleate dilution.

Fatty acid addition below the cmc

After reproducing the original matrix effect, we repeated the experiment of oleate addition to DOPC seed vesicles, but at a much lower oleate concentration. By adding oleate at a concentration below the cmc, we ensured that all oleate was added as monomers. The turbidity measurements are shown in Fig. 3. At time point zero, 10 μL of 22 mM oleate was added to 1 mL of water NaOH (pH 10; trace *A*). After ~1 min, 1 mL of 0.1 mM DOPC LUV (150 nm; pH 8.5) was added to this 1 mL of 0.2 mM oleate (pH 10) (final pH 8.5). Although the oleate concentration clearly is below the cmc (cmc of potassium oleate: 0.6 mM (33)), we conclude that new vesicles were formed, based on the scattering increase and the fact that the vesicles did not increase in size (the final vesicle size was 130 nm as probed by DLS). Control measurements show that the dilution of seed vesicles with water results in lower optical density (trace *B*), and that no increase in scattering occurred without the presence of the seed vesicles (trace *C*).

Excess fatty acids in the outer leaflet are the driving force for the formation of new vesicles

From a mechanistic point of view, one might expect that fatty acids added to seed vesicles initially would insert into the outer leaflet, leading to an instantaneous material excess in the outer leaflet with respect to the inner leaflet of the vesicles. Such a material excess in the outer leaflet with respect to the inner leaflet could then favor vesicle budding and possibly fission into smaller vesicles. This is because small vesicles have a larger ratio between the surface area of the outer leaflet and the surface area of the inner leaflet, and therefore would be better able to accommodate the larger surface area of the outer monolayer.

To test whether a process of membrane insertion resulting in excess material in the outer leaflet with respect to the inner leaflet of the vesicles indeed is likely to act as a driving force for vesicle deformation and subsequent splitting, we used two complementary approaches. First, we slowed down the rate of addition of new material to give the fatty acids time to flip from the outer leaflet to the inner leaflet, thereby counteracting the material imbalance. As illustrated in Fig. 4, slow addition over a period of 10 h led to growth of

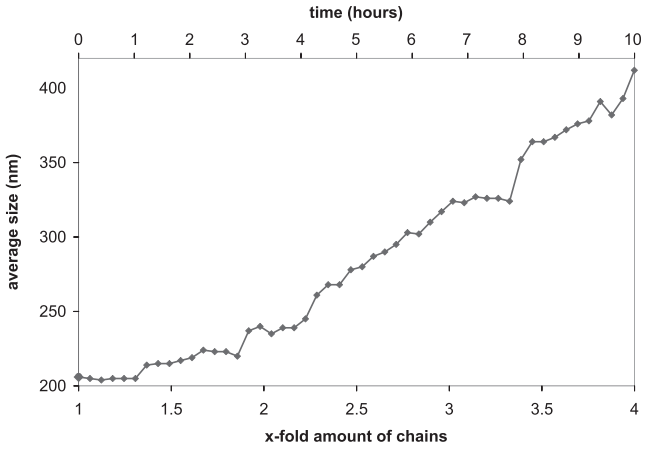

FIGURE 4 Effect of slowing down the rate of addition of oleate: the change in vesicle size determined by DLS was measured over time. In the time period of 10 h, a fourfold greater amount of chains was added continuously.

the vesicles. More precisely, Fig. 4 shows that a fourfold increase in the amount of chains resulted in vesicles with a double diameter, and hence in vesicles with a fourfold greater surface, convincingly demonstrating that fission did not take place. Second, we lowered the pH of the medium to increase the rate of flip of the fatty acids from the outer leaflet to the inner leaflet by decreasing the amount of negative charge (4,5,34). We found that lowering the pH from 8.5 to 7.9 resulted in a growth of the vesicle size by 25%, which is most likely due to a decrease of the material excess in the outer leaflet.

These results support the hypothesis that the standard procedure of instantaneously adding a severalfold excess of fatty acids to seed vesicles results in membrane insertion, leading to an initial imbalance of the fatty acid content in the two leaflets, which in turn results in budding and subsequent fission of the vesicles.

MD simulations of vesicle replication on fatty acid addition

To study in detail the possible pathways for the replication process of fatty acid vesicles upon the addition of new fatty acids to their exterior, we performed CG MD simulations. For these simulations we used a CG fatty acid model, which differs from the more common atomistic models in that the molecules consist of so-called CG particles that combine the average behavior of several atoms in one single particle. The advantage of coarse-graining is that the resulting system consists of fewer particles and larger time steps are allowed. This enables larger systems to be studied over larger time intervals. The CG fatty acid model (the derivation of which is described in Materials and Methods) is shown in Fig. 5 *A*. The initial configuration of our simulation is shown in Fig. 5 *C*. For clarity in this figure, the water, which is explicitly present in the simulations, is not shown. The initial configuration was created by adding new fatty acid molecules to the final stage of a previous simulation of a fatty acid vesicle. The fatty acids that constitute the preformed vesicle are colored gray, and the newly added fatty acids are colored red. Furthermore, the headgroups of the fatty acids are colored using a lighter tint than the hydrophobic tails, as illustrated in Fig. 5 *B*. It is important to note that the different colors for preexisting and new fatty acids are used simply to aid visualization of the simulations; all fatty acids interact in precisely the same way.

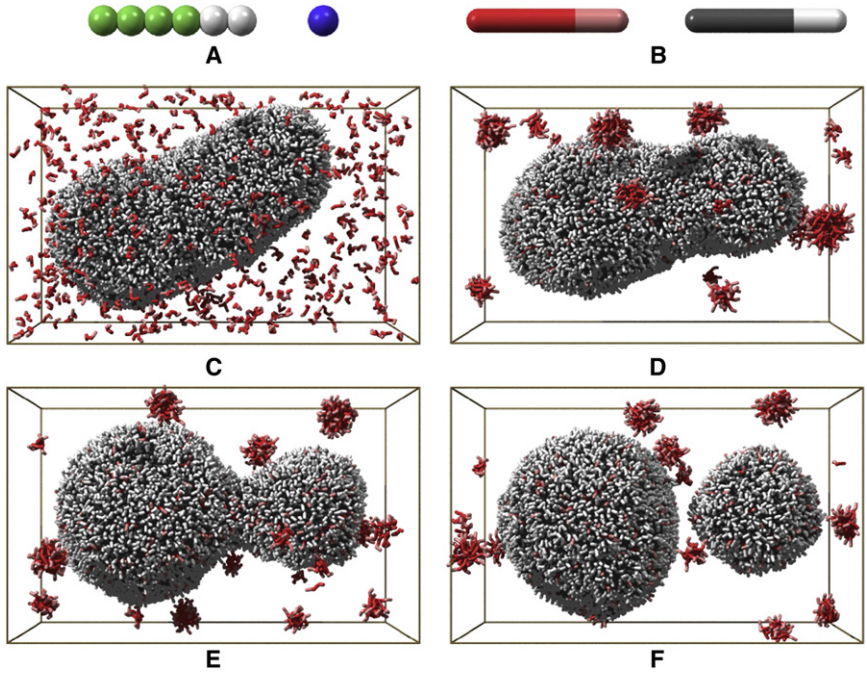

FIGURE 5 (*A*) CG fatty acid and water model. (*B*) Representation of the fatty acids used in frames *C–F* (gray for fatty acids in preformed vesicle, and red for freshly added fatty acids). (*C*) The initial configuration. (*D*) The final configuration of the first simulation. (*E*) An intermediate of the second simulation (iteration 1,100,000). (*F*) The final configuration of the second simulation.

To keep the simulation computationally feasible, the initial vesicle was chosen to be relatively small and prolate ellipsoid in shape. The ellipsoid shape was preferred because spherical vesicles cannot deform without first changing the membrane area to volume ratio. This volume ratio can only change by diffusion of water out of the vesicle or by membrane growth, and this would be costly in terms of computer time. The membrane of the preformed vesicle consists of 5935 fatty acids, of which 2028 are in its inner leaflet and 3907 in its outer leaflet. The vesicle, which contains 18,341 water particles in its interior, has an outer diameter of ~34 nm along its longest axis and 20 nm in the other two perpendicular directions.

We added the extra fatty acids by randomly placing them in the vesicle's exterior water phase and removing any overlapping water particles. After the addition of 500 fatty acids, the vesicle's exterior still contained 256,626 water particles, resulting in a total of 313,577 particles in the simulation.

The first simulation run consisted of 2,500,000 iterations. The randomly dispersed fatty acids in the initial configuration rapidly aggregate into micelles or are captured directly into the outer leaflet of the vesicles membrane. The micelles diffuse throughout the solution and grow in size as they fuse with each other. However, contrary to simulations of spontaneous vesicle formation where no preexisting vesicle is present, the micelles do not have the opportunity to grow large enough to form a new vesicle (28,35). Instead, the micelles are absorbed by the preexisting vesicle. The final configuration of this simulation is shown in Fig. 5 *D*. During the simulation, 144 of the newly added fatty acids fused with the vesicle, whereas the remaining 356 formed micelles. In each fusion event, all new fatty acids ended up in the outer leaflet of the vesicle's membrane. However, due to 26 flips of fatty acids from the outer to the inner leaflets of the membrane, at this stage the vesicle's membrane contained 2054 fatty acids in the inner and 4025 in the outer leaflet. Furthermore, the vesicle contained 18,361 waters in its interior, indicating that some water diffused through the membrane to the vesicle's interior.

Because both the diffusion of micelles and the likeliness of fusion with the vesicle decreases with increasing micelle size, we accelerated the process to save computational time by adding new fatty acids instead of waiting for the remaining micelles to eventually fuse with the vesicle. To this end, first the fatty acids that not yet fused with the vesicle were substituted by water particles. Subsequently, 500 new fatty acids were randomly dispersed in the exterior.

Using this configuration, we performed a new simulation. In the second simulation run, as in the first, part of the newly added fatty acids fused again, directly or as micelles, with the vesicle. Because all 201 new fatty acids that fused with the vesicle ended up again in the outer membrane leaflet and only 24 fatty acids flipped from the outer leaflet to the inner leaflet, the difference in number of fatty acids between the inner and outer leaflets increased further. The shape change due to this additional excess of fatty acids in the outer leaflet was much more prominent than in the first simulation run. First, a budded state was formed in which two rather spherical parts of the vesicle remained connected to each other via a neck (Fig. 5 *E*). Next, breakage of this neck resulted in vesicle fission, as can be seen in Fig. 5 *F*, which shows the final configuration (after 1,800,000 iterations). (An overview of all simulations is shown in Movie S1 in the Supporting Material.)

Deformation to the budded state is only a geometrical change, whereas for the breakage of the neck a topological change is also needed. This topological change is best seen in cross sections of the vesicle, as shown in Fig. 6. Part *A* of this figure shows the initial configuration of the second simulation run, and part *B* shows the budded intermediate where water is still present in the neck. The first stage of neck breakage includes the retreat of waters from this neck and the self-fusion of the inner monolayer. When the waters retreat from the neck, the vesicle's internal water content splits into two parts. The fatty acid headgroups in the neck's inner monolayer remain directed toward the water. As a result, the headgroups also split into two parts, whereas the tails of the fatty acids of these two groups around the breakage point are directed toward each other, filling the space where the waters used to be (Fig. 6 *C*). Subsequently, the two water compartments become more spherical, increasing the distance between these compartments, and thus also between the fatty acids of the inner monolayer that follow the water. At this stage the outer membrane leaflet also self-fuses, such that the connection between the two subvesicles is achieved purely by fatty acids from this outer leaflet. Breakage of this last connection completes the fission process (Fig. 6 *D*).

After full fission occurs, the two smaller vesicles that have formed together still contain 18,347 water particles. No additional exchange of water between the vesicle interior and exterior has taken place during fission, except for the usual diffusion of water over the membrane that was present during the whole simulation. The observed fission process is thus not leaky.

A control simulation was performed in which the preformed vesicle was simulated for the same period of time without the addition of new fatty acids. This vesicle maintained its initial shape. The largest change during the 4,300,000 iteration simulation was the net diffusion of 38 water particles toward the vesicle interior, which increased the interior water content by ~0.2%.

The vesicle deformations reported here are similar to those we observed in previous studies (30,32). However, in those studies the vesicle deformations resulted from changes in interaction parameters. When the interaction between lipid headgroups and solvent for the lipids in the inner and/or outer leaflet was changed, membrane packing changed and consequently spontaneous curvature was introduced in the bilayer, which resulted in the vesicle's deformation. In contrast, in the study presented here, the

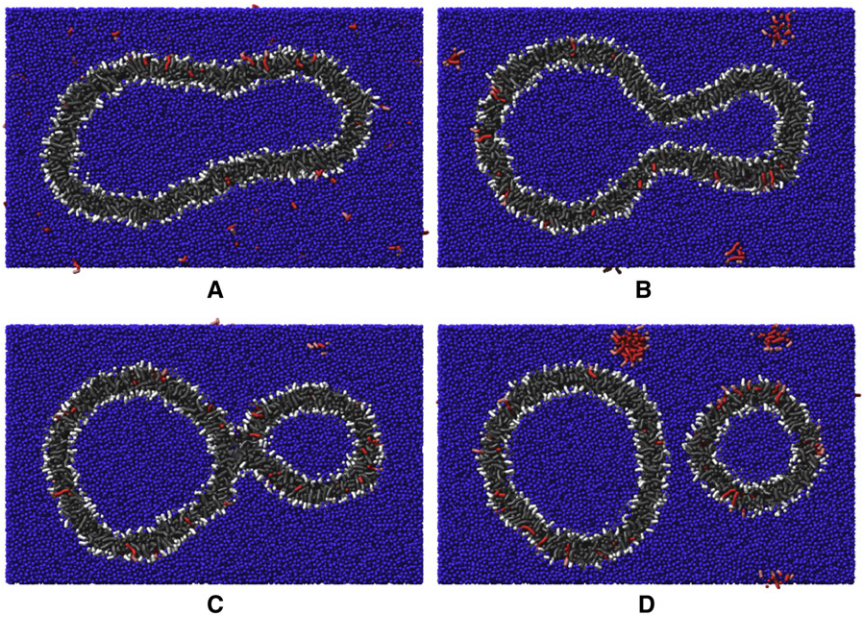

FIGURE 6 Cross-sectional views of intermediates of the second run: (*A*) the initial configuration, (*B*) iteration 1,100,000, (*C*) iteration 1,500,000, and (*D*) the final configuration.

interactions were identical for all fatty acids. Consequently, as there is no distinction between the molecules in the inner and outer leaflets, deformation of the vesicles should have another cause, namely, the change in the number of molecules in the two bilayer leaflets. When the newly added fatty acids fuse with the vesicle's membrane, they all are incorporated into the membrane's outer leaflet. Because the flip is slow compared to the absorption of new fatty acids, every additional fusion of a micelle with the vesicle increases the difference in the number of fatty acids between the inner and outer monolayers of the vesicle. The resulting difference in area between the inner and outer monolayers is then relieved by deformation of the vesicle.

DISCUSSION

By combining different experimental approaches with CG MD simulations, we obtained insights into the molecular mechanism underlying the so-called matrix effect (11,20). The main results of our experiments were that 1), we reproduced the matrix effect using a slightly different, homogeneous lipid system with DOPC as seed vesicles, and showed that upon oleate addition the average size of the newly formed vesicles is similar to the size of the seed vesicles; 2), the content of the seed vesicles does not leak out to the exterior during this process; 3), new vesicles are also formed when oleate is added as monomers; and 4), the size distribution can be controlled by changing the rate of oleate addition, and hence the rate of the transbilayer movement is a key factor in controlling the final vesicle size. Together these results suggest that the matrix effect is the consequence of a process in which vesicles first grow and then undergo fission. The CG simulations agree remarkably well with the results of these experiments. For example, the simulations showed that new vesicles were formed in the absence of seed vesicles, whereas in the presence of seed vesicles a process of vesicle replication occurred. Furthermore, the simulations showed that the replication process is not leaky, providing confidence that both approaches describe the same process.

With respect to the size of the final vesicles, not only do the techniques agree fairly well, they also provide new, complementary mechanistic insights. The first step in the fission process according to the MD simulations would be vesicle deformation due to spontaneous curvature as a result of insertion of fatty acids into the outer leaflet. Simulations have shown that vesicle deformation due to positive spontaneous curvature usually results in the formation of twin vesicles of approximately the same size (30,31). If the number of lipids in the inner leaflet were to remain the same before and after fission, this would lead to division into two identical daughter vesicles with a radius that would be decreased by 30% as compared to the size of the parent vesicle. However, the essence of the matrix effect (11) is that the size of the newly formed vesicles is similar to that of the seed vesicles. Hence, to maintain the same size distribution of the newly formed vesicles compared to the parent vesicles, some lipids must flip to the inner membrane. Therefore, a prerequisite for creating spontaneous curvature would be that the rate of flip must be slow compared to the rate of insertion of new material into the outer leaflet. Both the simulations and experiments indicate that this indeed is the case. Thus, together, the experiments and simulations provide a detailed mechanism for vesicle replication in which an imbalance of material across both leaflets and slow lipid flip-flop are key features.

Of course, there are also differences between the experiments and the simulations. For example, in the simulation

system, the sizes and time intervals remain small compared to the those in the experimental setting. As a consequence of the relatively short time span that can be simulated, both the diffusion of water over the membrane and the growth of the membrane are limited. To let a sufficient amount of new lipids fuse with the vesicle to make it deform, a very high concentration of newly added fatty acids is applied and the starting vesicle is elongated. Due to the same limitation of computational time, the preexisting vesicle in the simulation is relatively small (with outer diameters of 34 and 20 nm) compared to experimental vesicles. However, continuum models of vesicle deformation show that the deformations of vesicles are independent of scale. When the vesicle radius is twice as large, the membrane area will be four times as large, and hence a fourfold area difference between the inner and outer monolayers is needed to obtain the same shape deformation. Hence, the ratio between the number of molecules to be added and the number of molecules originally present in the membrane is constant. Simulations starting with a larger preexisting vesicle are thus expected to give similar results when the number of lipids added increases with the same factor, but again at the expense of more computational power. Thus, all main results from the experiments are in correspondence with the fission pathway observed in the simulations in molecular detail.

Further experimental evidence that the rate of new material insertion is large enough to create spontaneous curvature was provided by two studies of the Szostak group. In kinetic Förster resonance energy transfer experiments, Chen and Szostak (15) showed that upon the addition of micelles to seed vesicles, the membranes of the seed vesicles grew ~40% within the first second after micelle addition. Bruckner et al. (36) showed that the relaxation of oleate membranes with a mismatch in inner and outer leaflet density takes several seconds. Together these findings indicate that upon micelle addition, membrane growth and buildup of spontaneous curvature can indeed go hand in hand. Furthermore, there is a limited growth of the vesicle interiors on this timescale. This is because even though the water permeability is high, the increased water content of the vesicle interior leads to an osmotic difference, and as a result the rate of volume increase is controlled by the low permeability of the membrane to solutes such as ions and buffer. In combination with this limited growth of the vesicle interior, the membrane expansion and buildup of spontaneous curvature allow the fission process to occur.

The experiment with the addition of oleate below the cmc shows that micelles are not required for the matrix effect to occur, which supports the leaflet mismatch-driven growth-fission pathway. However, our experiments do not rule out the possibility that catalyzed growth of new membranes can occur as well when high concentrations of fatty acid micelles are added.

What is the implication of these results for the possible role of the matrix effect in early life? The results suggest that an outside supply of fatty acids that insert into the outer leaflet of a prebiotic vesicle could result in vesicle replication without leakage of contents, but it would require a flip rate that is low compared to the insertion rate. This might be accomplished by a relatively high pH in the outside medium. However, such a mechanism is probably not relevant for early life, where one would expect membrane material to be added as a result of metabolic processes from the inside of the primitive cell. Our results suggest that the process we describe in this study of creating excess material in the outer leaflet of the bilayer, which in the end results in vesicle replication without leakage, might then still be accomplished, but under two conditions: 1), the rate of insertion of new material into the inner leaflet of the membrane is slow as compared to the rate of flop to the outer leaflet; and 2), the flop rate is much higher than the rate of flipping back to the inner leaflet. The latter condition might be accomplished simply by having a relatively low pH inside and a relatively high pH outside. Testing this hypothesis experimentally, however, will remain a major technical challenge.

SUPPORTING MATERIAL

One movie is available at http://www.biophysj.org/biophysj/supplemental/S0006-3495(10)00801-5.

REFERENCES

1. Luisi, P. L., P. Walde, and T. Oberholzer. 1999. Lipid vesicles as possible intermediates in the origin of life. *Curr. Opin. Colloid Interface Sci.* 4:33–39.
2. Hanczyc, M. M., and J. W. Szostak. 2004. Replicating vesicles as models of primitive cell growth and division. *Curr. Opin. Chem. Biol.* 8:660–664.
3. Walde, P. 2006. Surfactant assemblies and their various possible roles for the origin(s) of life. *Orig. Life Evol. Biosph.* 36:109–150.
4. Deamer, D. W. 2008. Origins of life: how leaky were primitive cells? *Nature.* 454:37–38.
5. Mansy, S. S., J. P. Schrum, …, J. W. Szostak. 2008. Template-directed synthesis of a genetic polymer in a model protocell. *Nature.* 454: 122–125.
6. Cistola, D. P., D. Atkinson, …, D. M. Small. 1986. Phase behavior and bilayer properties of fatty acids: hydrated 1:1 acid-soaps. *Biochemistry.* 25:2804–2812.
7. Cistola, D. P., J. A. Hamilton, …, D. M. Small. 1988. Ionization and phase behavior of fatty acids in water: application of the Gibbs phase rule. *Biochemistry.* 27:1881–1888.
8. Gebicki, J. M., and M. Hicks. 1973. Ufasomes are stable particles surrounded by unsaturated fatty acid membranes. *Nature.* 243:232–234.
9. Morigaki, K., and P. Walde. 2007. Fatty acid vesicles. *Curr. Opin. Colloid Interface Sci.* 12:75–80.
10. Fukuda, H., A. Goto, …, P. Walde. 2001. Electron spin resonance study of the pH-induced transformation of micelles to vesicles in an aqueous oleic acid/oleate system. *Langmuir.* 17:4223–4231.
11. Blochliger, E., M. Blocher, …, P. L. Luisi. 1998. Matrix effect in the size distribution of fatty acid vesicles. *J. Phys. Chem. B.* 102:10383–10390.
12. Lonchin, S., P. L. Luisi, …, B. H. Robinson. 1999. A matrix effect in mixed phospholipid/fatty acid vesicle formation. *J. Phys. Chem. B.* 103:10910–10916.

13. Berclaz, N., M. Muller, …, P. L. Luisi. 2001. Growth and transformation of vesicles studied by ferritin labeling and cryotransmission electron microscopy. *J. Phys. Chem. B.* 105:1056–1064.

14. Berclaz, N., E. Blochliger, …, P. L. Luisi. 2001. Matrix effect of vesicle formation as investigated by cryotransmission electron microscopy. *J. Phys. Chem. B.* 105:1065–1071.

15. Chen, I. A., and J. W. Szostak. 2004. A kinetic study of the growth of fatty acid vesicles. *Biophys. J.* 87:988–998.

16. Chungcharoenwattana, S., and M. Ueno. 2004. Size control of mixed egg yolk phosphatidylcholine (EggPC)/oleate vesicles. *Chem. Pharm. Bull. (Tokyo).* 52:1058–1062.

17. Chungcharoenwattana, S., H. Kashiwagi, and M. Ueno. 2005. Effect of preformed egg phosphatidylcholine vesicles on spontaneous vesiculation of oleate micelles. *Colloid Polym. Sci.* 283:1180–1189.

18. Chungcharoenwattana, S., and M. Ueno. 2005. New vesicle formation upon oleate addition to preformed vesicles. *Chem. Pharm. Bull. (Tokyo).* 53:260–262.

19. Mavelli, F., and P. L. Luisi. 1996. Autopoietic self-reproducing vesicles: a simplified kinetic model. *J. Phys. Chem.* 100:16600–16607.

20. Rasi, S., F. Mavelli, and P. L. Luisi. 2003. Cooperative micelle binding and matrix effect in oleate vesicle formation. *J. Phys. Chem. B.* 107:14068–14076.

21. Rasi, S., F. Mavelli, and P. L. Luisi. 2004. Matrix effect in oleate micelles-vesicles transformation. *Orig. Life Evol. Biosph.* 34:215–224.

22. Rogerson, M. L., B. H. Robinson, …, P. Walde. 2006. Kinetic studies of the interaction of fatty acids with phosphatidylcholine vesicles (liposomes). *Colloids Surf. B Biointerfaces.* 48:24–34.

23. Stano, P., E. Wehrli, and P. L. Luisi. 2006. Insights into the self-reproduction of oleate vesicles. *J. Phys. Condens. Matter.* 18:S2231–S2238.

24. Walde, P., R. Wick, …, P. L. Luisi. 1994. Autopoietic self-reproduction of fatty-acid vesicles. *J. Am. Chem. Soc.* 116:11649–11654.

25. Thomas, C. F., and P. L. Luisi. 2004. Novel properties of DDAB: matrix effect and interaction with oleate. *J. Phys. Chem. B.* 108:11285–11290.

26. Hanczyc, M. M., S. M. Fujikawa, and J. W. Szostak. 2003. Experimental models of primitive cellular compartments: encapsulation, growth, and division. *Science.* 302:618–622.

27. Luisi, P. L., T. P. de Souza, and P. Stano. 2008. Vesicle behavior: in search of explanations. *J. Phys. Chem. B.* 112:14655–14664.

28. Markvoort, A. J., K. Pieterse, …, P. A. Hilbers. 2005. The bilayer-vesicle transition is entropy driven. *J. Phys. Chem. B.* 109:22649–22654.

29. Smeijers, A. F., A. J. Markvoort, …, P. A. Hilbers. 2006. A detailed look at vesicle fusion. *J. Phys. Chem. B.* 110:13212–13219.

30. Markvoort, A. J., R. A. van Santen, and P. A. J. Hilbers. 2006. Vesicle shapes from molecular dynamics simulations. *J. Phys. Chem. B.* 110:22780–22785.

31. Markvoort, A. J., P. Spijker, …, P. A. Hilbers. 2009. Vesicle deformation by draining: geometrical and topological shape changes. *J. Phys. Chem. B.* 113:8731–8737.

32. Markvoort, A. J., A. F. Smeijers, …, P. A. Hilbers. 2007. Lipid-based mechanisms for vesicle fission. *J. Phys. Chem. B.* 111:5719–5725.

33. Verko-Antonovich, I. Yu., L. R. Ziganshina, A. P. Rakhmatullina, and R. A. Akhmed'yanova. 2004. Surface activity of fatty acid salts in aqueous solutions. *Russian J. Appl. Chem.* 77:595–598.

34. Kamp, F., and J. A. Hamilton. 1992. pH gradients across phospholipid membranes caused by fast flip-flop of un-ionized fatty acids. *Proc. Natl. Acad. Sci. USA.* 89:11367–11370.

35. Goetz, R., and R. Lipowsky. 1998. Computer simulations of bilayer membranes: self-assembly and interfacial tension. *J. Chem. Phys.* 108:7397–7409.

36. Bruckner, R. J., S. S. Mansy, …, J. W. Szostak. 2009. Flip-flop-induced relaxation of bending energy: implications for membrane remodeling. *Biophys. J.* 97:3113–3122.